

Tunable Bandgap in Graphene by the Controlled Adsorption of Water Molecules

Fazel Yavari, Christo Kritzinger, Churamani Gaire, Li Song, Hemtej Gulapalli, Theodorian Borca-Tasciuc, Pulickel M. Ajayan, and Nikhil Koratkar*

Graphene, a single-atom-thick layer of sp^2 -hybridized carbon atoms, has generated considerable excitement in the scientific community due to its peculiar electronic band structure, which leads to unusual phenomena such as the anomalous quantum Hall effect,^[1,2] spin-resolved quantum interference,^[3] ballistic electron transport,^[4] and bipolar supercurrent.^[5] However, pristine graphene is a semimetal with zero bandgap; the local density of states at the Fermi level is zero and conduction can only occur by the thermal excitation of electrons.^[2] This lack of an electronic bandgap is the major obstacle limiting the utilization of graphene in nano-electronic and -photonic devices,^[6,7] such as p–n junctions, transistors, photodiodes, and lasers.

The graphene band structure is sensitive to lattice symmetry and several methods have been developed to break this symmetry and open an energy gap. These methods are based on a variety of techniques, such as defect generation,^[8] doping (e.g., with potassium^[9]), applied bias,^[10–12] and interaction with gases^[13] (e.g., nitrogen dioxide). For instance, in reference [12] a tunable bandgap of up to 0.25 eV was achieved for electrically gated bilayer graphene by a variable external electric field. Similarly, an internal electric field produced by an imbalance of doped charge between two graphene layers has been shown to open a bandgap.^[9] It has been demonstrated that a gap of ≈ 0.26 eV can be produced by growing graphene epitaxially on silicon carbide substrates.^[14] This gap originated from the breaking of sublattice symmetry due to the graphene–substrate interaction. Patterned adsorption of atomic hydrogen onto the Moiré superlattice positions of graphene^[15] has resulted in a bandgap of ≈ 0.73 eV opening, while half-hydrogenated graphene^[16] resulted in a bandgap of ≈ 0.43 eV. A graphene nanomesh structure^[17] has also been shown to exhibit a bandgap. In this graphene structure, lateral quantum confinement and localization effects due to

edge disorder, such as variable edge roughness, was proposed as the mechanism responsible for the bandgap opening.

In this Communication, we report a facile technique to open a bandgap in graphene based on water adsorption to the graphene surface. An environmental chamber with precise control of the absolute humidity level is used to control the amount of water adsorbed to the graphene surface. A bandgap of ≈ 0.206 eV can be opened by simply exposing the sample to an absolute humidity level of ≈ 0.31 kg kg⁻¹ (i.e., 0.31 kg of water per 1 kg of dry air) in an environmental chamber. The effect is reversible and the bandgap reduces to ≈ 0.029 eV in vacuum. This technique does not require any complicated engineering or modification of the graphene surface and does not rely on chemical doping or defect generation. It should be noted that humidity can be precisely controlled only in a confined space and this has important implications for device implementation. However, with rapid advances in micropackaging of micro-electromechanical (MEMs) devices, it is relatively straightforward to pattern such microenclosures,^[18,19] which could be used in different parts of the chip/device. Graphene is a zero-bandgap material, which limits its utility. So, any process that induces a bandgap (in specific parts of the circuit by different amounts or over the whole circuit by the same amount) would make it a relevant semiconducting material.

Graphene samples were synthesized by chemical vapor deposition (CVD) on copper (Cu) foil using hexane as a liquid precursor.^[20] After growth, a thin poly(methyl methacrylate) (PMMA) film was coated on the graphene/Cu substrate. The underlying Cu substrate was dissolved in dilute HNO₃ and the film was transferred onto a Si substrate with a ≈ 300 -nm-thick insulating SiO₂ layer. Photolithography followed by e-beam evaporator deposition was used to pattern four electrodes (Ti/Au, 3/30 nm) on the top surface of the transferred graphene film. As indicated in the optical micrograph of **Figure 1a**, the electrodes were deposited at four points to form a Van Der Pauw configuration.^[21] Scanning electron microscopy (SEM) imaging of the sample (bottom inset in Figure 1a) indicates a $\approx 30 \mu\text{m} \times 16 \mu\text{m}$ region of the graphene film that is enclosed within the electrode pattern. We characterized this region of the graphene film by atomic force microscopy (AFM). There is evidence of folds or wrinkles on the film surface (top inset in Figure 1a); this is probably an artifact of the process used to transfer the graphene film from the Cu foil to the SiO₂ substrate. Raman spectroscopy using 514-nm-wavelength excitation was used to

F. Yavari, C. Kritzinger, C. Gaire, Prof. T. Borca-Tasciuc, Prof. N. Koratkar
Department Mechanical
Aerospace and Nuclear Engineering
Rensselaer Polytechnic Institute
Troy, NY 12180, USA
E-mail: koratn@rpi.edu

L. Song, H. Gulapalli, Prof. P. M. Ajayan
Department of Mechanical and Materials Engineering
Rice University
6100 Main Street, Houston, TX 77005, USA

DOI: 10.1002/sml.201001384

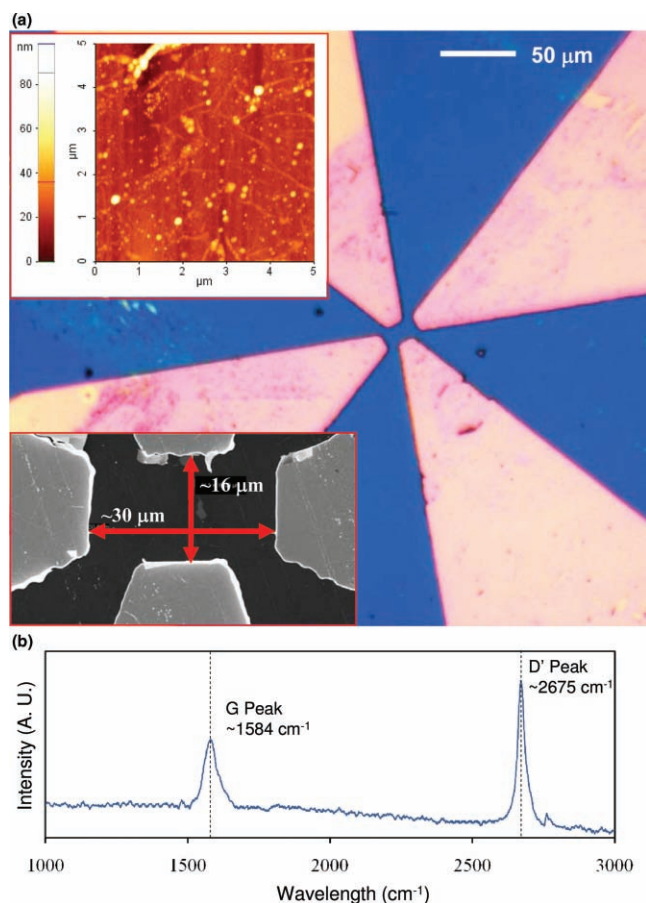


Figure 1. a) Optical image of the graphene sheet and contact electrodes in the Van Der Pauw configuration on a Si wafer with a ≈ 300 -nm-thick SiO_2 coating. Top inset shows topography of the graphene film obtained using AFM; the film is not perfectly flat and displays some wrinkling. The bottom inset shows an SEM image of the electrode configuration with graphene film dimensions of $\approx 30 \mu\text{m} \times 16 \mu\text{m}$ within the electrode pattern. b) Raman spectroscopy characterization of the graphene film showing the measured G and D' band peaks.

record the G and D' peaks of the graphene film (Figure 1b). The ratio of the intensities of the G and D' modes was ≈ 0.5 , which indicates ≈ 1 – 2 graphene layers within our film.^[22,23]

Connecting the gold contact pads of the Van Der Pauw configuration to the measurement setup was a challenge. Since the pads were very thin and smooth, standard wire bonding peeled off the contact pads and could not be used. Also, a conventional probe station could not be utilized since the majority of the measurements needed to be performed inside an environmental chamber and the probe station could not be installed within the chamber. Therefore, we utilized silver epoxy (EJ-2189 two part kit from EPOXY Technology) which has a low Ohmic contact resistance of less than 0.001% of the sheet resistance of the graphene sample. Using four gold wires and silver epoxy, the contact pads shown in Figure 1a were connected to four leads of a conventional chip carrier, making it possible to electrically address the sample. For the resistivity measurements reported here, first the sheet resistance is calculated using two (standard and reversed polarity) measurements for each of the vertical and horizontal resistances^[21] associated with the Van Der

Pauw configuration. The vertical and horizontal resistances are estimated as the averages of these two measurements. The advantage of using both standard and reversed polarity and obtaining the resistance from the slope of the voltage versus current curves is that any offset voltages are eliminated. After obtaining the vertical and horizontal resistances, the sheet resistance is obtained by using the Van Der Pauw formula.^[21] Then, the sheet resistivity is computed from the measured sheet resistance and the film thickness. To expose the graphene film to different amounts of water vapor, the sample was placed within an environmental chamber. The environmental chamber has two temperature controllers, one to control the dry-bulb temperature and another to control the wet-bulb temperature. The absolute humidity level in the chamber can be inferred from these two temperatures. The same absolute value of humidity can be obtained for many different combinations of the dry-bulb and wet-bulb temperatures. We used this effect to our advantage to study the activation energy of the graphene film at each absolute humidity value.

Prior to beginning the hydration experiments, the resistivity of the graphene sample was measured in vacuum. Then, it was exposed to four different levels (0.022, 0.065, 0.152, and 0.312 kg of water per kg of air) of absolute humidity inside the chamber. For each value of humidity, the change in the film resistivity was measured as a function of time (Figure 2a). As seen in this figure, the adsorption of water to the graphene surface is a relatively slow process and it takes several hours for the resistivity to saturate at each humidity level. In Figure 2b, we plot the effect of the absolute humidity on the saturated value of the graphene film resistivity and the time taken to achieve 90% of the saturation resistivity. The graphene resistivity shows a nonlinear dependence on the absolute humidity (H) and increases as $\approx H^{0.25}$. Conversely, the time to achieve 90% of the saturated resistivity decreases with increasing humidity as $\approx H^{(-0.25)}$. Thus, the rate of adsorption of water molecules to the graphene surface is affected by the absolute humidity level and, once the number density of water molecules on the graphene surface has stabilized, the resistivity value also saturates. Note that the absolute change in the resistivity can be as large as $\approx 150\%$ (i.e., ≈ 2.5 -fold increase) for the case of 0.312 kg of water vapor per 1 kg of dry air.

To establish whether the sensitivity of the graphene sheet's resistivity to humidity is caused by the opening of a bandgap in the material, we varied the temperature in the environmental chamber while keeping the absolute humidity constant. By varying temperature, we can determine if there exists an activation energy (a direct measure of bandgap in intrinsic semiconductors)^[24,25] associated with electron transport in the graphene sheet. While optical methods, such as angle-resolved photoemission spectroscopy (ARPES), are typically used to study band structure, in our case, the sample was confined within the environmental chamber and so ARPES could not be used; we therefore used the activation-energy method to estimate the bandgap. After keeping the graphene film inside the humidity chamber for sufficient time (Figure 2) to assure the saturation condition, the change in electrical resistance of the graphene film as a function of

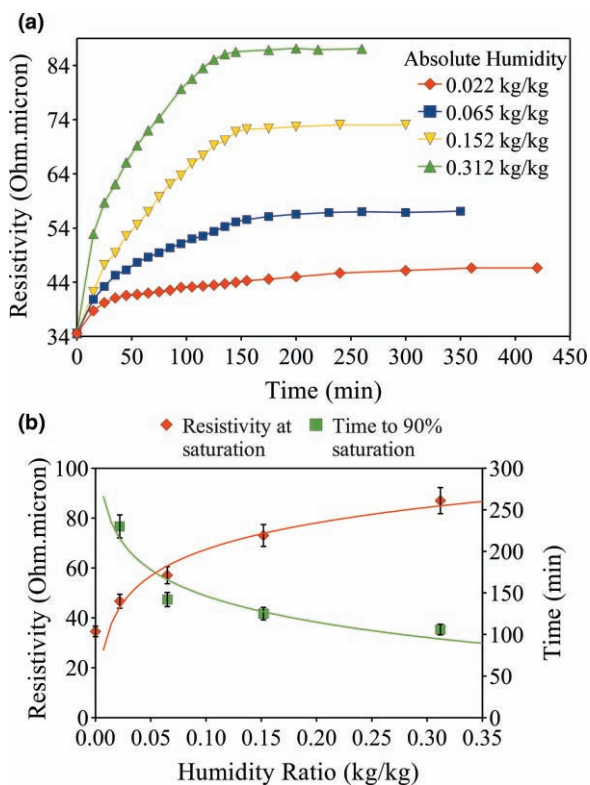


Figure 2. a) Resistivity-versus-time characteristics of graphene film for different values of absolute humidity. b) The values of maximum resistivity observed and the time taken to achieve 90% of the saturation value for different values of absolute humidity. The graphene film's resistivity is increased by increasing the absolute humidity while the time to saturation decreases with increasing humidity.

temperature was measured at four different values (0.022, 0.065, 0.152, and 0.312 kg kg⁻¹) of absolute humidity inside the chamber. The temperature was varied from 300 to 370 K; this was the widest range of temperatures for which the humidity level could be kept constant within the chamber. In **Figure 3a**, we show the Arrhenius plot (logarithm of film conductivity versus inverse of temperature)^[24,25] for different values of absolute humidity. It is evident that the Arrhenius plot is a straight line, the slope of which yields an activation energy or bandgap in the sample. Another possibility is that the increase in the graphene film's conductivity with temperature (Figure 3a) may be an indirect effect resulting from temperature-induced desorption of water from the surface. This latter possibility appears unlikely for a number of reasons. First, we find that the time constants involved in water adsorption/desorption for our graphene film are of the order of several hours (Figure 2). By contrast, for the temperature tests in Figure 3a, the film resistivity jumped to a stable value within few minutes (which is the time taken for the temperature in the environmental chamber to stabilize at the new setting). Second, even in vacuum (where there is no issue of water adsorption/desorption), the conductance change with temperature stabilized within minutes identical to the cases with humidity. Thirdly, the temperature difference between any two adjacent data points in Figure 3a is $\approx 4^\circ$. It is unlikely that a significant conductivity change

will arise from water desorption induced by a 4° rise in temperature.

In Figure 3b, we plot the measured bandgaps obtained from Figure 3a for different values of absolute humidity in the chamber. For zero humidity in the chamber, the graphene film shows a nonzero bandgap of ≈ 0.029 eV. This is probably an artifact of impurity scattering, which may create a small nonzero bandgap even in the absence of humidity or due to substrate interactions.^[14,27] As the absolute humidity level is increased, the measured bandgap increases sharply following a $\approx H^{0.33}$ dependence and saturates at about ≈ 0.206 eV at a humidity level of ≈ 0.312 kg kg⁻¹. Note that this effect is reversible; when the humidity level was reduced back to zero, the bandgap dropped back to ≈ 0.029 eV. This was confirmed several times by repeated cycling of the humidity level in the 0–0.312 kg kg⁻¹ range. These experiments were also repeated for different graphene samples and the results were reproducible.

The opening of the gap may be a result of the breaking of the sublattice and molecular symmetries of graphene by the adsorbed water molecules. Chakraborty and coworkers^[26] have studied the effect of adsorption of water molecules on the band structure of graphene using spin-polarized density functional theory. Their simulations indicate that clusters

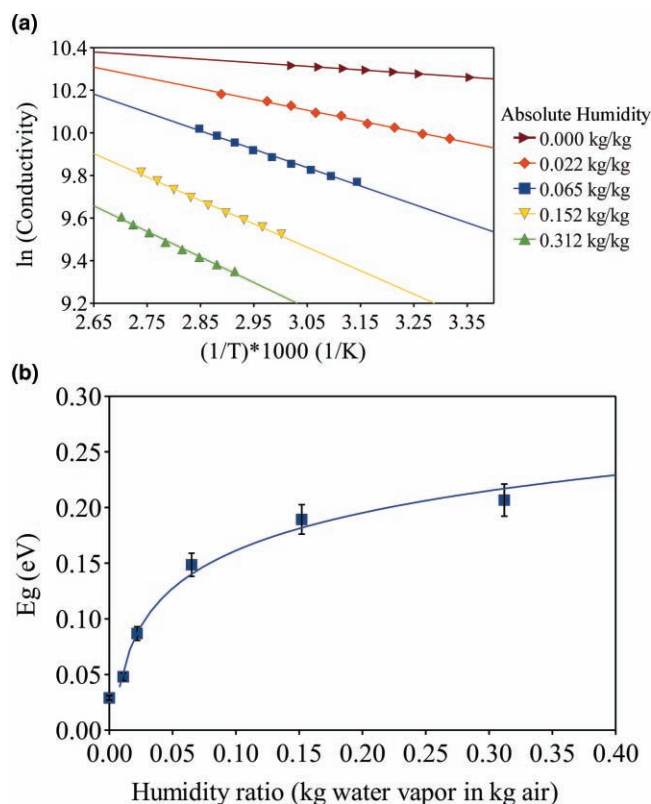


Figure 3. a) Arrhenius plot for the graphene-film conductivity plotted with respect to the inverse of the operating temperature for different values of absolute humidity. The activation energy (i.e., bandgap) is derived from the slope of the Arrhenius plot. b) The bandgap (E_g) is plotted as a function of the absolute humidity. The bandgap increases sharply with humidity and then saturates at a level of ≈ 0.206 eV for a humidity level of ≈ 0.312 kg kg⁻¹.

of water molecules act as defects that repel the wave functions of the molecular orbitals corresponding to the α -spin and β -spin states to the opposite (zigzag) edges of the nanoscale graphene sheet; this breaks the symmetry and results in a large bandgap. The magnitude of the gap was found to be very sensitive to the interaction of the graphene surface with water; depending on whether the dipole moment of the adsorbed water molecules was aligned perpendicular or parallel to the graphene surface, the bandgap was found to vary between 2.0 and 0.8 eV. In our case, the measured bandgap is significantly lower (≈ 0.2 eV). The graphene film used in our experiments is $\approx 30 \mu\text{m} \times 16 \mu\text{m}$ in size, much larger than the graphene of several nanometers in scale studied in reference [26]. Confinement, edge effects, and chirality have significant influence on nanoscale graphene and, therefore, a direct quantitative comparison of our results with the theoretical calculations in reference [26] are not meaningful. A study using density-functional calculations that may be more relevant to our experiments was performed by Wehling and co-workers,^[27] in which they investigated the electronic properties of free-standing graphene, as well as graphene on SiO₂ substrates, with and without water adsorption. They found the role of defects in the SiO₂ substrate to be crucial. The dipole moments of H₂O adsorbates cause local electrostatic fields that can shift the substrate's defect states with respect to the graphene electrons and cause doping. Coupling with surface defects in the SiO₂ substrate may explain why we measure a bandgap of ≈ 0.029 eV even in vacuum (with no water adsorption). Wehling and coworkers^[27] also report that the hybridization of substrate defect states with the graphene bands can be reduced by H₂O in between the graphene and the SiO₂ substrate. This is also a likely scenario in our experiments since the graphene film has significant wrinkles or folds (Figure 1a) and water molecules can infiltrate into the spaces between the graphene film and the SiO₂ substrate.

To summarize, we have demonstrated that a tunable bandgap of up to ≈ 0.206 eV can be engineered in graphene by the controlled adsorption of water molecules to the surface of graphene. This method does not require any complicated modifications to the graphene sheet or complex configuration of the layers. However, the device will have to be equipped with an enclosure(s) to precisely control the humidity levels. The hydration of the graphene film (and hence the bandgap) can be tuned by controlling the absolute humidity level of the environment.

Acknowledgements

N.K. and P.M.A. acknowledge funding support for this research from the advanced energy consortium (AEC). T.B-T acknowledges

support from NRI/NIST. L.S. is supported by DOE-BES program DE-SC0001479 for the sample growth and device fabrication.

- [1] K. S. Novoselov, A. K. Geim, S. V. Morozov, D. Jiang, M. I. Katsnelson, I. V. Grigorieva, S. V. Dubonos, A. A. Firsov, *Nature* **2005**, *438*, 197.
- [2] Y. Zhang, Y.-W. Tan, H. L. Stormer, P. Kim, *Nature* **2005**, *438*, 201.
- [3] M. B. Lundeberg, J. A. Folk, *Nat. Phys.* **2009**, *5*, 894.
- [4] M. S. Wijeratne, Y. Zhang, U. C. Coskun, W. Bao, C. N. Lau, *Science* **2007**, *14*, 1530.
- [5] H. B. Heersche, P. J. Herrero, J. B. Oostinga¹, L. M. K. Vandersypen, A. F. Morpurgo, *Nature* **2007**, *446*, 56.
- [6] O. C. Compton, S. T. Nguyen, *Small* **2010**, *6*, 711.
- [7] J. A. Lin, D. Teweldebrhan, K. Ashraf, G. X. Liu, X. Y. Jing, Z. Yan, R. Li, M. Ozkan, R. K. Lake, A. A. Balandin, C. S. Ozkan, *Small* **2010**, *6*, 1150.
- [8] X. C. Dong, Y. M. Shi, Y. Zhao, D. M. Chen, J. Ye, Y. G. Yao, F. Gao, Z. H. Ni, T. Yu, Z. X. Shen, Y. X. Huang, P. Chen, L. J. Li, *Phys. Rev. Lett.* **2009**, *102*, 135501.
- [9] T. Ohta, A. Bostwick, T. Seyller, K. Horn, *Science* **2006**, *313*, 951.
- [10] E. Rudberg, P. Salek, Y. Luo, *Nano Lett.* **2007**, *7*, 2211.
- [11] Y.-W. Son, M. L. Cohen, S. G. Louie, *Nature* **2006**, *444*, 347.
- [12] Y. B. Zhang, T. T. Yang, C. Girit, Z. Hao, M. C. Martin, A. Zettl, M. F. Crommie, Y. R. Shen, F. Wang, *Nature* **2009**, *459*, 820.
- [13] S. Y. Zhou, D. A. Siegel, A. V. Fedorov, A. Lanzara, *Phys. Rev. Lett.* **2008**, *101*, 086402.
- [14] S. Y. Zhou, G. H. Gweon, A. V. Federov, P. N. First, W. A. De Heer, D. H. Lee, F. Guinea, A. H. C. Neto, A. Lanzara, *Nat. Mater.* **2007**, *6*, 770.
- [15] R. Balog, B. Jorgensen, L. Nilsson, M. Andersen, E. Rienks, M. Bianchi, M. Fanetti, E. Laegsgaard, A. Baraldi, S. Lizzit, Z. Slijivancanin, F. Besenbacher, B. Hammer, T. G. Pedersen, P. Hofmann, L. Hornekaer, *Nat. Mater.* **2010**, *9*, 315.
- [16] J. Zhou, M. M. Wu, X. Zhou, Q. Sun, *Appl. Phys. Lett.* **2009**, *95*, 103108.
- [17] J. Bai, X. Zhong, S. Jiang, Y. Huang, X. Duan, *Nat. Nanotechnol.* **2010**, *5*, 190.
- [18] R. Ramesham, R. C. Kullberg, *J. Microlith. Microfab. Microsyst.* **2009**, *8*, 031307.
- [19] R. M. Shahriar, M. M. Chitteboyina, D. P. Butler, Z. Celik-Butler, S. P. Pacheco, R. V. McBean, *J. Microelectromech. Syst.* **2010**, *19*, 911.
- [20] A. Srivastava, C. Galande, L. Ci, L. Song, C. Rai, D. Jariwala, K. F. Kelly, P. M. Ajayan, *Chem. Mater.* **2010**, *22*, 3457.
- [21] L. J. Van Der Pauw, *Philips Res. Rep.* **1958**, *13*, 1.
- [22] D. Graf, F. Molitor, K. Ensslin, C. Stampfer, A. Jungen, C. Hierold, L. Wirtz, *Nano Lett.* **2007**, *7*, 238.
- [23] A. Gupta, G. Chen, P. Joshi, S. Tadigadapa, P. C. Eklund, *Nano Lett.* **2006**, *6*, 2667.
- [24] L. Solymar, D. Walsh, *Electrical Properties of Materials*, Oxford University Press, New York **1998**.
- [25] J. D. Livingston, *Electronic Properties of Engineering Materials*, John Wiley & Sons, New York **1999**.
- [26] J. Berashevich, T. Chakraborty, *Phys. Rev. B* **2009**, *80*, 033404.
- [27] T. O. Wehling, A. I. Lichtenstein, M. I. Katsnelson, *Appl. Phys. Lett.* **2008**, *93*, 202110.

Received: August 10, 2010
Revised: August 27, 2010
Published online: